Designing a multi-channel continuous perfusion system for 3D blood vessel-on-chip with viscous finger patterning

Yuki Nagatomo

Supervised by: Prof. dr.ir. M. Odijk, Prof. dr. A.D. Van der Meer, and H. H. T Goosen-Middelkamp (MSc)

***Abstract*—Cardiovascular disease is one of the leading cause of deaths worldwide, but there has yet to be an efficient method for drug testing, with animal testing being both unethical and unrepresentative of human physiology. Recent advancements in research on Vessel-on-Chip (VoC) devices open up the possibility for in vitro drug testing. However, these microfluidic devices do not have a method to culture multiple cells in a 3D accurate environment under continuous perfusion. This paper discusses the challenges of VoC systems and evaluates 2 existing perfusion mechanisms - the UniChip and standardized fluidic circuit board (FCB). Calculations and electrical equivalent circuits were made to analyze the system. The results revealed challenges for the UniChip design in parallelization of the channels because high hydraulic resistances are required in the supporting channels to obtain desired shear rates. On the contrary, the standardized approach of the FCB shows more promise due to many existing examples for parallelization and continued development of microfluidic building blocks. In the long run, this approach should allow for a simplified method of research applications and automation due to the ease of integrating sensors and additional components. The paper also addresses the challenges with the viscous finger patterning technique and fabrication of the chip that should be considered to move forwards with designing an appropriate perfusion system.**

I. Introduction

According to the World Health Organization (WHO), approximately 17.8 million of 55.4 million deaths worldwide in 2019 are due to cardiovascular causes. This number amounts to 32% of all deaths of which coronary artery disease and strokes contribute to more than half of these deaths with 8.8 million and 6.2 million deaths respectively and are the two leading causes of death for the past two decades [1].

While research is being conducted to find effective treatment for such diseases, the current method of testing for the later phases, animal testing, is inefficient since animals do not fully reenact human physiology [2] and is fundamentally unethical. With recent advancements in stem cell-based organ-on-chip platforms, in vitro systems can act as an improvement to current drug testing methods and can furthermore be used to better understand the various phenomena of the human body.

Organ-on-a-Chip is a microfluidic device with microengineered *in vitro* structures that allows the physiology and pathology of human organs to be replicated and experimented upon [3][4][5]. Several papers have shown that 2D vascular networks can be cultured in conventional 2D tissue culture dishes, however, there is not sufficient evidence to demonstrate that such system is suitable for in vitro representation [6][7]. As such, 3D vascular systems show more promise to be physiologically and pathologically accurate for experimentation.

Currently there are two main methods to generate reproducible lumens. The first being patterning the extracellular matrix (ECM) of the channels with a small-diameter needle [8][9]. Although reliable, the labor-intensive nature of this method is not sustainable for large-scale experiments [10]. The second method, which will be the method focused on in this paper, is using a technique called viscous finger patterning (VFP). This microfluidic technique uses a fluid to displace a more viscous fluid in a channel to create a finger-like shape in the middle of the channel [11][12]. This can be seen in figure 1 [10]. By conducting VFP with a less viscous medium on a channel with hydrogel, the 3D lumen of interest can be constructed. However, this width of the resultant lumen is dependent on various factors including ECM concentration and pH, timing, pressure, and channel geometries [10], hence fabricating such channels with precision is an important aspect for high throughput. The method for which these chips are being constructed is through creating master-molds by micro milling Poly(methyl methacrylate) (PMMA), which are later used to conduct soft lithography with Polydimethylsiloxane (PDMS) to produce the chips of interest.

While much progress has been made with engineering effective techniques to create these channels, a perfusion system to keep these parallelized 3D channels under continuous flow during cell culturing and experimentation has not been developed. This paper aims to evaluate existing perfusion techniques and propose a viable method in keeping the 3D lumens under continuous flow.

II. Problem definition and research questions

This research aims to answer the question ”How can we design a multi-channel continuous perfusion system for 3D blood vessel-on-chip with viscous finger patterning?”. There are 3 main components in this research question that need to be analysed and taken into consideration during the design process.

A. Parallelization of channels

Firstly, the parallelization of channels is important for preparing multiple channels of the same environments to improve the replicability of experiments and the throughput per chip [13].

Currently, experiments are carried out on a chip with 3 parallelized channels each with the dimension of $500\,\mu\mathrm{m} \times 500\,\mu\mathrm{m} \times 1\,\mathrm{cm}$, spaced equal distance from one another and placed on on a 75mm x 25mm x 1mm microscope glass.

Therefore, maintaining the same number of parallel channels would be highly preferred. The reason for having 3 parallelized channels instead of more is due to the speed limitation of manually viscous finger patterning each individual channel.

B. Keeping multiple channels under equal pressure and shear distribution

Keeping these channels under equal pressure and shear distribution is arguably the most challenging and important aspect of this research.

Shear stress is one of the 2 important forces exerted when blood is pumped from the heart and can be interpreted as the frictional force from the blood flow parallel to the vessel wall. The other important force is exerted by blood pressure stretching the wall. Such forces are sensed by cells making up the vessel wall to modulate endothelial structure and functions [14][15], hence play a big role in maintaining normal vascular functions. Additionally, continuous flow is required in the cell culturing process to improve cell survivability [16], hence a system that can operate for several days without human interjection will be ideal.

Furthermore, characterization of channel shear rate and flow rate is an important aspect of application. Research published by Costa et al. observed the effect of arterial thrombosis by observing the backflow velocity at the area of platelet aggregation [2]. Therefore, designing the system for a standardized shear rate is important for experiments and future applications.

In this paper, the specification for channel shear rate is set at $1000s^{-1}$, as this value was a physiological standard identified from expert interviews.

C. Incorporating the viscous finger patterning technique to the chip design

Lastly, VFP is required for creating 3D lumens since it is the most efficient way of reproducing the in vitro models of the vessels of interest. VFP was a microfluidic technique generated from when a "finger-like" shape, also known as the Saffman-Taylor finger [17], was discovered through the middle of the channel when a less viscous fluid displaces a more viscous fluid. This microfluidic technique is demonstrated in figure 1 [10].

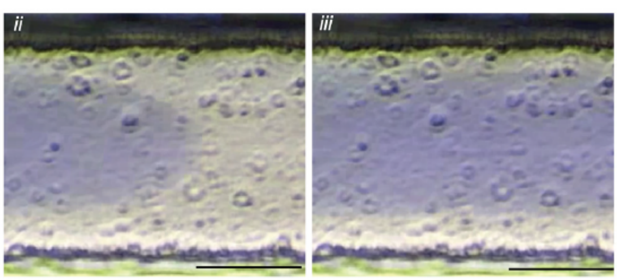

Fig. 1: Demonstration of the Saffman-Taylor finger and lumen formation[10]

Currently, the extended passive pumping (EPP) protocol is proven to be the most reliable method of VFP [10]. This method combines passive pumping method developed by Bischel et al. [11] and the gravity driven protocol developed by Herland et al. [12]. The passive pumping method utilizes the differential surface tension of the different diameter droplets placed at the inlet and outlet, but lumen formed with this method characteristically decreased in diameter across the channel due to the entry effect [11]. On the other hand, the gravity driven method relies on the hydrostatic pressure of the chip inlet through placing a pipette tip at the inlet to extend the pathway, and had a increasing lumen diameter towards the end [12]. The EPP takes the characteristics of both by inserting pipette tips of 7mm in both inlets, which resulted in the lowest variance amongst the 3 methods [10], and this protocol as well as channel dimensions are being used today.

Several points to be careful of when incorporating the VFP into the design is the possibility of air-bubbles which lead to imperfect lumen formation. This has been reported by Herland et al. [12] and have been circumvented by inserting pipette tips prior to injecting the hydrogel [10]. However, this can be an issue if no precaution is taken. Another issue that was identified through conversations with users is the collapsing of hydrogel. Since all the formerly introduced protocol uses the same inlet and outlet for inserting the hydrogel and the less viscous medium, there was no issue regarding this. However, in the case that there are several inlets or with a greater/slower flow rate, there is a risk for the lumen to collapse at more vulnerable junctions of the channel. The collapsing of lumen has already been reported with the GD protocol when insufficient pressure was applied, to which de Graaf et al. has speculated to be due to the result of batch-to-batch differences [10]. Therefore, experimentation and fabrication technique should be also be considered.

The goal of the research is to evaluate existing perfusion methods for VoC systems, and propose a viable design for the 3D application.

III. Method and Results

A. Expert Interviews

Expert interviews were conducted alongside initial literature research in order to grasp a better understanding of the topic and existing designs. Furthermore, it was a valuable opportunity to discuss possible implementation with experts who have been working in the field for many years.

A major takeaway from the expert interviews was learning about the existing designs that the experts have worked on. While the implementation was for different applications, information attained from the interviews elaborated on prior literature research on pneumatic valves and implementation using multilayered fluidic circuit board design. It also clarified uncertainties in assembly and perfusion pumps used in practice.

Additionally, there was common consensus that SolidWorks simulations are better suited for the scope of this research instead of using the COMSOL software. This was due to the time limitation and the rapid prototyping that creating models in SolidWorks allow for, since the files for micromilling have to be designed in this software. Furthermore, the learning curve for COMSOL is steep, therefore, it was decided to use SolidWorks as the main software for design and simulations due to my prior experience with it.

During the expert interviews, 2 notable designs were mentioned. The first design that was a more straightforward approach using gravity-driven recirculation which was the UniChip design. The second design was the fluidic circuit board which involved the use of valves. Taking into consideration the time restrictions of this assignment, the UniChip design was investigated first because it was considered an easier design to replicate and print using the micro-milling machine.

B. *UniChip Design*

The UniChip design was proposed by Wang et al., as a means of incorporating vasculature and other shear stress-sensitive tissues to in vitro microfluidic systems and achieve a continuous unidirectional flow [18]. The design is based from a pumpless gravity-driven platform using a rocking motion by Sung et al. [19], which has been later adapted for many other OOC models [20][21][16].

The chip consists of 1 channel of interest, denoted as C_u, and supporting channels, A and B, which connects C_u to 2 reservoirs, as shown in figure 2. Tubular channels are used to connect channel B with the respective reservoirs that acts as passive valves using capillary forces [18]. When placed on the rocking table which was programmed to flip quickly between ± 18 degrees every 15 second intervals, the fluid will flow from reservoir 1 to a_1 and divide into channels a_2 and C_u. The fluid passing through channel C_u will then flow through b_2 into reservoir 2. The passive valves restrict any flow from the inlet of channel B from reservoir 1 as long as the tilt in the rocking table does not exceed the capillary force, and the hydraulic resistance are equal throughout each respective supporting channels [18].

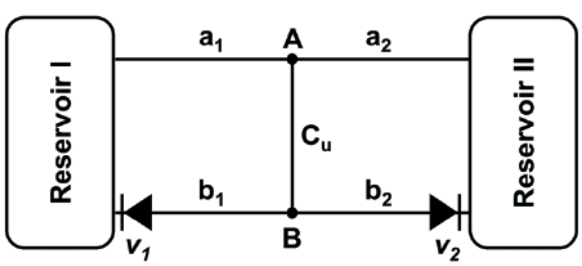

Fig. 2: Schematic Design of UniChip [18]

To analyze the operation of the chip from an electrical engineering perspective, the system was expressed as its electrical equivalent as shown in figure 3. The rocking table acts as an effort source which generates a hydraulic pressure due to the difference in the height of the 2 reservoirs. The reservoir itself acts as a compliance element expressed as a capacitor, from which the flow is generated, and is connected in series with the voltage source. Therefore, the capacitor and voltage source can be expressed as a charged capacitor or battery. Each channel acts as a resistance due to the hydraulic resistances in the channel, and the passive valves are simply diodes. The electrical equivalent circuit demonstrates an inverse exponential decay as the charged up capacitor discharges over time. Depending on the hydraulic resistances, fluid water level, and the frequency of which the rocking table tilts, this exponential behavior may not be observed and therefore can be simplified as a voltage source.

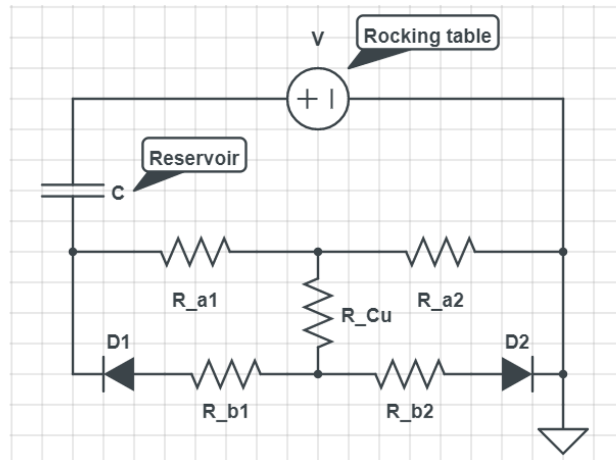

Fig. 3: Electrical Equivalent of single channel UniChip [18]

The UniChip is constructed by assembling 5 upper layers that make up the reservoir and supporting channels with a lower layer that acts as the housing for channel C_u with screw-to-expand inserts. The upper layers and housing cover is cut from PMMA sheets with only the cell culture layer fabricated with silicon[18]. The cell culture layer is attached to a plastic cover slip. This assembly therefore allows for the VFP to be done manually before assembling with the top layer. This is shown in Figures 4 and 5.

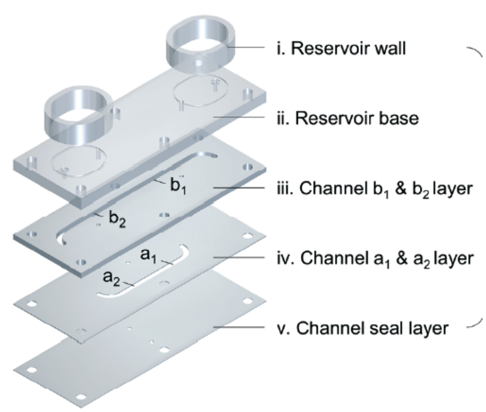

Fig. 4: Top layer assembly of UniChip [18]

To evaluate the feasibility of the design, a MATLAB script was made to calculate the necessary channel dimensions to achieve a shear rate of $1000s^{-1}$ while keeping the channel dimensions that are typically used for 3D blood vessel research which is $500\,\mu\mathrm{m} \times 500\,\mu\mathrm{m} \times 1\,\mathrm{cm}$ [10].

The channel dimensions are related to fluid flow and pressure according to the following equations: Firstly the pressure drop between the input and output of each channel can be

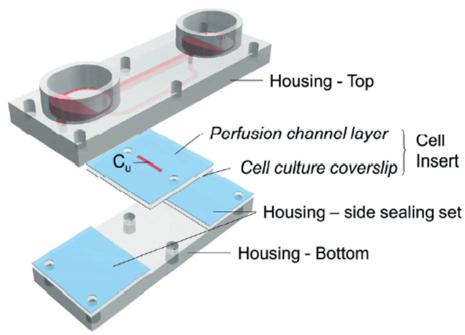

Fig. 5: Top and Bottom layer assembly of UniChip [18]

expressed by the sum of the flow rate multiplied by the hydraulic resistance for the path the fluid flows. This gives a system of equation as shown [18]:

$$\begin{cases} \Delta P_{I_1 I_3} = Q_{a_1} R_{a_1} + Q_{a_2} R_{a_2} \\ \Delta P_{I_1 I_4} = Q_{a_1} R_{a_1} + Q_{C_u}(R_{C_u} + R_{b_2}) \\ Q_{a_1} = Q_{a_2} + Q_{C_u} \end{cases} . \tag{1}$$

where P is the pressure difference in the input and output of the reservoirs, Q denotes the flowrate, and R the hydraulic resistance. Furthermore, the pressure drop can also be expressed as follows [18]:

$$\Delta P = \rho g \Delta h \tag{2}$$

where ρ is the fluid density, g is the gravitational acceleration, and δh is the difference in height of the input and output points on the reservoir.

Next, the equations for the hydraulic resistance are shown at equation 3, where μ is the dynamic fluid viscosity, and w, h, l points to the width height, and length of the channel respectively [18]. The tubular equation is used to calculate hydraulic resistance for channel C_u since the channel will undergo VFP to form 3D lumen.

$$\begin{cases} R_{rectangular} = \frac{12\mu l}{wh^3}[1 - \frac{192h}{\pi^5 w} tanh(\frac{\pi w}{2h})]^{-1} \\ R_{tubular} = \frac{8\mu L}{\pi r^4} \end{cases} . \tag{3}$$

Furthermore, the shear stress is calculated using 2 different equations for the supporting channel and VFP channel for the same reason [18][10]:

$$\begin{cases} \tau_{rectangular} = \frac{6\mu Q}{wh^2} \\ \tau_{tubular} = \frac{32\mu Q}{pid^3} \end{cases} . \tag{4}$$

Since the design specifications aim for a shear rate of $1000s^{-1}$, the equation that correlates shear rate and shear stress is [22]:

$$\tau = \mu \cdot \gamma \tag{5}$$

Several assumptions were made during the calculation. Firstly, the channel diameter of C_u was defined as 250 µm, taking reference to the average reported diameter for the VFP protocol used [10]. Additionally, the dynamic fluid viscosity (μ) and the fluid density (ρ) both assume the values of water at 35 °C to mimic body temperature. Furthermore, the angle of tilt table for calculating the elevation and capillary force was defined as 18 degrees, following the angle used by Wang et al [18].

The MATLAB script first calculated and compared the values for fluid flow and shear stress reported by Wang et al. While the values did not match up completely since the paper calculated the dimensions using viscosity and fluid density values at 20 degrees to validate the design with experiments in the lab, a similar flow and shear was obtained from the calculations. The MATLAB script also calculated the supporting channel dimensions required to obtain a shear rate of $1000s^{-1}$ with the current dimensions being used for VoC research [10]. During this, it was assumed that the difference in length of channel A and B will be kept the same as that in the paper by Wang et al., 11mm, and the width and length will follow similar values as well [18]. As a result, the required length increased to 33.8mm for a_1 and a_2, and 44.8mm for b_1 and b_2. Compared to the 15.3mm and 26.3mm used by Wang et al. [18] this is a significant increase. This suggests that the larger the length of channel C_u, the larger the supporting channels need to be such that channels A and B have higher resistances, and ideal shear rate is obtained.

To understand how much the dimensions influence the shear rate in the channels, the shear rate was plot for varying channel dimensions. Figure 6 shows a plot of shear rate against varying channel length. According to equation 3, the relationship is linear. The plot is linear and shows a steep slope, indicating that tuning this parameter will change the shear rate significantly. In addition to the length, the height and tilt angle was also investigated and can be found in the appendix A, alongside comments and realizations from the plots.

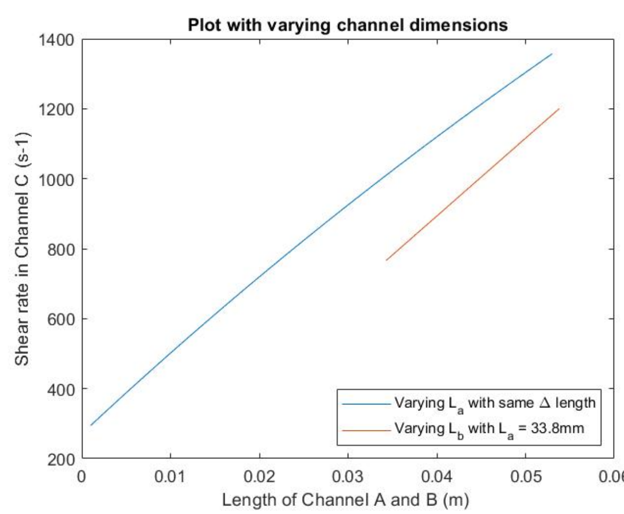

Fig. 6: Plot of Shear rate for varying channel length for A (blue) and B (red)

After the calculations were completed, a preliminary design was made in SolidWorks based on the calculated parameters with the plan to print and carry out experiments (Appendix B). However, the UniChip design has additional challenges when trying to parallelize the channels. Wang et al. proposes a generalized design (Figure 7) for the UniChip where multiple channels can be parallelized between 2 reservoirs, however, one critical requirement is that the system requires a minimum of 1 active or passive valve at each inlet/outlet of channel B [18]. This requirement to have at least 2 valves in the system does not pose a large challenge since the passive valve utilizing hydraulic resistance should suffice. However, the viscous finger patterning step can cause the system to not reach the ideal shear rate if each channel have unequal or uneven lumen diameters. This is difficult to control since VFP is currently conducted by hand and lumen formation remains to be inconsistent.

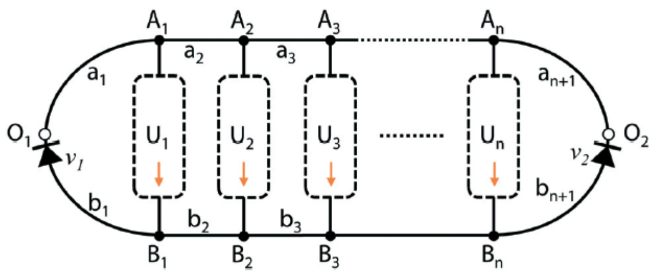

Fig. 7: Proposed design for parallelized UniChip design [18]

Alike the single channel UniChip design, the parallelized system was expressed as its electrical equivalent circuit in figure 8. The operation of the system is alike that of the single channel, but with the circuit acting as a current divider. With proper design considerations to keep each parallel resistances equal through adjusting the resistance values in channels a and b, the current across the channels of interest should remain equal.

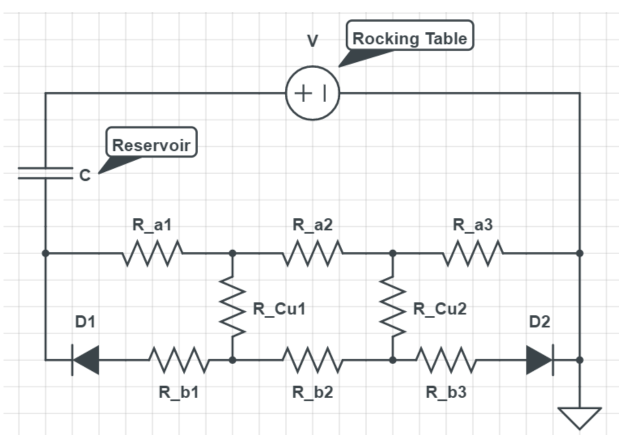

Fig. 8: Electrical Equivalent of parallelized UniChip [18]

The MATLAB script for the calculations with annotations can be found in the appendix D.

C. Fluidic Circuit Board with valves

Since the UniChip design faced a challenge in parallelization which is one of the requirements in the research question, the fluidic circuit board method of implementation was considered.

In efforts to establish a standardized format for designing microfluidic chips, microfluidic building blocks (MFBBs) were realized [23][24]. These building blocks are analogous to transistors and switches in the electrical engineering field [25], and instead of reinventing the wheel for every research application, these building block allows for a simplified design cycle where only the fluidic circuit board (FCB) has to be designed [23].

Realizing a system for 3D VoC using MFBBs will allow for easy implementation of future design iterations or improvements, since it uses standardized components. Vollertsen et al. has successfully demonstrated the application of a MFBB enabler which allowed a better standardized plug-and-play protocol with 64 parallelized chambers in 2D. This enabler and FCB design successfully operated with a microfluidic large-scale integration (mLSI) MFBB and a dosing MFBB [13]. For this implementation, with the use of selective coating, only the channels of interest should undergo VFP to recreate the appropriate environment for 3D lumens, which is not possible by only including a VFP step to the suggested cell culturing protocol. This is because VFP requires the channels to be filled with hydrogel for the less viscous fluid to displace the existing hydrogel and create an appropriate lumen.

A suggestion that was made during the expert interview was to create a separate channel that can be opened or closed using pneumatic valves where VFP can be done. This applies the multiplexer logic used in the mLSI MFBB of Vollertsen et al. which can be seen in figure 9. The mLSI MFBB incorporates pneumatic valves in "push-up" configuration and allowing control over the perfusion of all 64 individual channels using multiplexer logic. Specifically Figure 9d shows the pressurization of the 4 bottom horizontal channels, which closes 3 of the valves allowing for 1 channel to remain open. By applying combinatorial logic, Vollertsen et al. has designed an MFBB with 8 control channels that controls 64 chambers individually [13].

The diagram for a possible implementation is shown in figure 10. This idea involves using 2 input channels to introduce the hydrogel and medium for VFP separately. The solid lines with dark valves will be the channel which will be opened first to introduce the hydrogel to all respective channels. Then, the dark valves will be closed, and light valves on the dotted lines will be used to conduct VFP by introducing the medium. This input channel will also be used for any further experiments. The medium input channel will be introduced from a higher layer of the chip instead of from the horizontal direction in order to prevent any lumen failure or collapse during VFP.

This diagram has been expressed in terms of electrical equivalent circuit as shown in figure 11. The valves are expressed as switches since they will only be used in fully open or closed configuration. Furthermore, both the input sources and control for the switch are voltage sources because one of the biggest assumption of the system is the use of one single Fluigent pressure pump for all operations due to its easily programmable 8-channel-pumpinng function. To achieve equal flow rate in each lumen channel, the medium

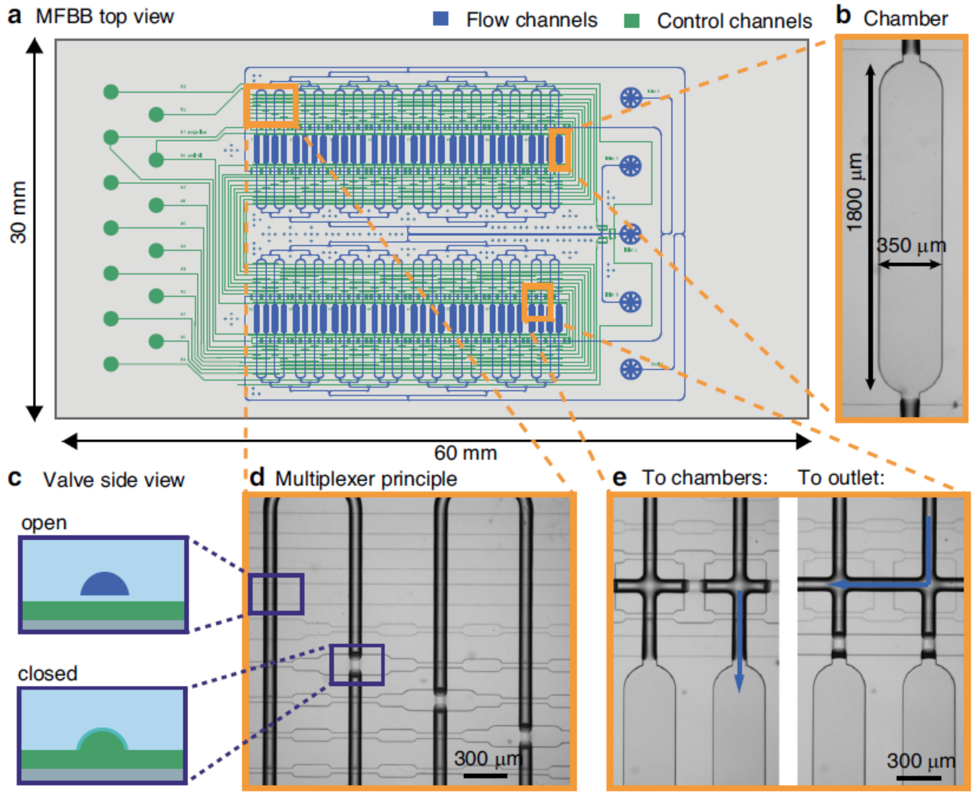

Fig. 9: mLSI Microfluidic Building Block enabling plug-and-play integration of 64 channel fluidic circuit board [13]

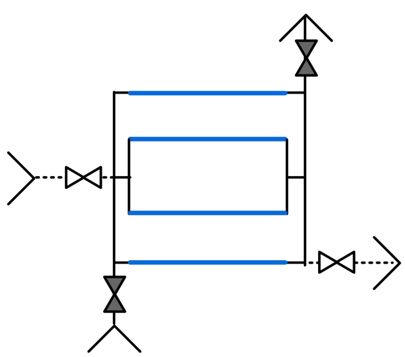

Fig. 10: Diagram of a possible implementation of VFP in FCB

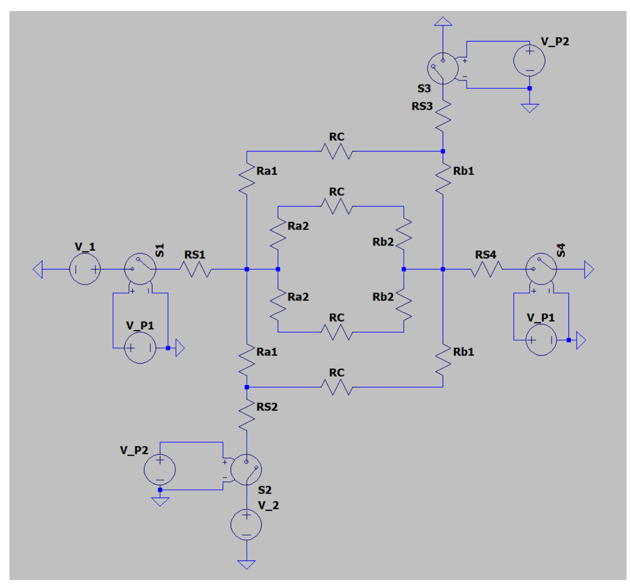

Fig. 11: Electrical equivalent circuit of a possible implementation of VFP in FCB

input or V1 of the equivalent circuit is placed at the middle of the system such that it is a symmetrical system apart from the hydrogel channel (V2). By choosing the proper channel dimensions for inner and outer channels, the resistance will be equal (Ra1 = Ra2, Rb1 = Rb2 in Figure 11), and the channel of interest highlighted in the blue area of figure 10 (or RC in Figure 11) will have equal flow across it.

Another possible implementation is to use valves in each channel to control the flow rate. This will allow for the user to account for any discrepancies in the lumen formation by adjusting the flow rate of each channel to achieve equal flow, or close off any channels with failed lumens. This possible implementation is shown in the appendix C

While this is a novel design, research to characterize VFP across multiple parallelized channels through one input channel has not yet been conducted. However, general characterization of the VFP shows dependency on various factors including density of the fluid, and mobility ratio to name a few [26]. Therefore, any discrepancy in the hydrogel and fluid flow in each channel may lead to inconsistent lumen diameter with multiple parallelized channels. Furthermore, pneumatic valves using a pressure pump only exist in an open configuration [27], which means, the valves connecting the hydrogel channel needs to be kept pressurized in order to remain closed.

IV. Discussion

A. UniChip

From the calculations, the required length for the desired shear stress was 33.8mm and 44.8mm for each of the 2 supporting output channels. While Wang et al. has also suggested a method for parallelization (Figure 7) [18], the resistance of each supporting channel will decrease due to the length of the channels being shortened as shown in figure 6. The main channel will have the same dimensions with a relatively high resistance, hence the flow rate will be lower, and attaining the required shear rate will be more difficult. Additionally, while the capillary rise should prevent any backflow, boundary conditions between each channel will change due to parallelization and its effects may affect the flow rate and edge effects may be observed. Furthermore, from expert interviews, it was identified that the viscous finger patterning was inconsistent with varying lumen diameter. Therefore, since the design relies on hydraulic resistance of the channels, this inconsistency will likely demonstrate discrepancies in shear rate between each channel.

Another thing to consider is that if any one of the lumen collapses, there is no option to remove that specific channel from the parallelized system since every supporting channel is connected to one another. This may be avoided by integrating a pneumatic valve to each channel, but this will require both a rocking table and a pressure pump to run and will be very inefficient. Furthermore, closing a channel will double the hydraulic resistance since it will extend the supporting channel by twice the length, and cause further problems.

B. Fluidic Circuit Board with Quake valves

The fluidic circuit board design faces a major challenge with viscous finger patterning. Because the device uses standardized components, a MFBB using the pressure pumps to conduct VFP through active pumping, as opposed to the current EPP protocol [10], would be ideal. This is because the FCB allows multiple channels to be parallelized and therefore manually conducting VFP across every one of the channels will be time consuming and undesirable due to the volatility of cell culturing environment. However, there is little progress in this specific field of study. One of the points to investigate is whether the VFP technique can be used in a multi-channel setup. This will be further discussed as a challenge with VFP under the next section.

While there are challenges, the FCB is the most promising design since it is a standardized method and can be expected to become more common in the future, alike that of electrical circuit and components. This would reduce the need for redesigning setups for certain drug testing and experiments, but rather apply a pre-existing MFBB someone has developed to accomplish the specific research application.

Furthermore, using pressure pumps allows for automation since many of said devices can be programmed. An issue with automation is introducing new resistances to the circuit. This was mentioned during expert interviews, and was verified during a test setup where the performance of a Fluigent pressure pump was investigated. During testing, the channel with a flow sensor attached had a significantly lower flow rate with the same pressure applied.

C. Other considerations

a) Viscous finger patterning: While the interfacial instability that is applied in the viscous finger patterning technique for VoC have been studied by many, it is a phenomenon that is very difficult to control. Various papers have attempted to do so through passive and active means [28]. Therefore, the complexity of investigating and realizing a effective protocol for promising designs such as the FCB will be a large challenge by itself.

While conducting viscous finger patterning across a singular channel will not be an issue, the idea of designing a MFBB to conduct VFP across parallelized channels might face different issues since the fluids will tend to travel the route with least resistances. If the VFP is implemented as figure 10, whether the lumen will form throughout all channels is yet to be verified. Since the length of the channel used for VoC research is 1cm long, it might be a challenge. Furthermore, there has not been any documentation that implemented the viscous finger patterning of VoC channels by means of active pumping discovered during this research.

b) Fabrication method: Another thing to consider when designing the systems is constructing a reliable protocol for assembling the different layers together. During the expert interviews, it was mentioned that leakage across the different layers is a common problem. For the approach of UniChip and FCB alike, several of the layers were combined using ethanol assisted thermal bonding and the entire chip was held together with screw-to-expand inserts or screwing nuts and bolts into the clamps [18][13]. Furthermore, preparation for cell culture also needs to be taken into consideration. A common step is to functionalize the surface through exposure to oxygen plasma [13]. This is an important step for VFP when introducing the collagen into the channels, hence being able to conduct that on channels of choice may be important depending on the chip design and purpose.

V. Conclusion

This paper investigated methods to design a multi-channel continuous perfusion system for 3D VoC research using viscous finger patterning. Parallelization of channels are important for throughput and upscaling of resarch, and continuous perfusion are important for cell survivability and maintaining normal vascular function of the cells. Therefore, systems were evaluated for a shear rate of $1000s^{-1}$, chosen as a physiological standard based on expert interviews. Furthermore, as a method for recreating physiological and pathologically accurate microfluidic systems, VFP was the method of choice to form 3D accurate lumens.

2 promising designs for 3D VoC perfusion systems were evaluated through calculations and modelling of electrical equivalent circuits, and its applicability was discussed. The UniChip by Wang et al. [18] utilized a rocking table for its a passive gravitational driven approach, however, due to the selected dimensions for the lumen channel, the supporting channels and required hydraulic resistances were too large. Additionally, due to VFP being inconsistent in its lumen diameter and with the added risk of the lumen collapsing, the system is not robust enough for paralellization. The FCB with MFBBs [13][25][23] shows better promise due to readily available standardized components. However, this still requires a standardized protocol for viscous finger patterning to be conducted since there is a lack of research and documentation for this multi-channel application.

In conclusion, designing a fluidic circuit board with microfluidic building blocks would allow for standardizing of perfusion systems in the long run and is the most optimal method of implementation. For this, better characterization of the viscous finger patterning technique is required.

VI. Acknowledgements

I would like to thank my supervisory committee, Prof. dr.ir. M. Odijk, Prof. dr. A.D. Van der Meer, and H. H. T Goosen-Middelkamp (MSc) for the opportunity to work on this assignment and all the kind support throughout the assignment. Additionally, I would like to thank A.G. de sa Vivas, A. R. Vollertsen, and E. Bossink for providing great insights during the expert interviews.

References

[1] WHO. Global health estimates: Leading causes of death.

[2] P. F. Costa, H. J. Albers, and J. E. A. Linssen et al. Mimicking arterial thrombosis in a 3d printed microfluidic in vitro vascular model based on computed tomography angiography data. *Lab Chip*, 17(2785), July 2017.

[3] S. N. Bhatia and D. E. Ingber. Microfluidic organs-on-chips. *Nature Biotechnol.*, 32:760–772, August 2014.

[4] A. D. van der Meer and A. van den Berg. Organs-on-chips: breaking the in vitro impasse. *Integr. Biol*, 4(461), March 2012.

[5] A. D. van der Meer, V. V. Orlova, and P ten Dijke et al. Three-dimensional co-cultures of human endothelial cells and embryonic stem cell-derived pericytes inside a microfluidic device. *Lab Chip*, 13(18):3562–8, May 2013.

[6] P. N. Silwinska, K. Alitalo, and E. Allen et al. Consensus guidelines for the use and interpretation of angiogenesis assays. *Angiogenesis*, 21(3):425–532, 2018.

[7] M. Simons, K. Alitalo, and B. H. Annex et al. State-of-the-art methods for evaluation of angiogenesis and tissue vascularization. *Circ. Res.*, 116:e99–e132, 2015.

[8] J. A. J. Torres, S. L. Peery, and K.E. Sung et al. Lumenext: A practical method to pattern luminal structures in ecm gels. *Adv. Healthcare Mater*, 5(2):128–204, 2012.

[9] A. Hasan, A. Paul, and A. Memic et al. A multilayered microfluidic blood vessel-like structure. *Biomed. Microdev*, 17(88), 2015.

[10] M. N. S. de Graaf, A. Cochrane, and F. E. van den Hil et al. Scalable microphysiological system to model three-dimensional blood vessels. *APL Bioengineering*, 3(026105), June 2019.

[11] L. L. Bischel, S. H. Lee, and D. J. Beebe. A practical method for patterning lumens through ecm hydrogels via viscous finger patterning. *Journal of Laboratory Automation*, 17:96–103, 2012.

[12] A. Herland, A. D. van der Meer, and E. A. FitzGerald et al. Distinct contributions of astrocytes and pericytes to neuroinflammation identified in a 3d human blood-brain barrier on a chip. *PLoS ONE*, 11(e0150360), 2016.

[13] A. R. Vollertsen, D. de Boer, and S. Dekker et al. Modular operation of microfluidic chips for highly parallelized cell culture and liquid dosing via a fluidic circuit board. *Microsystems & Nanoengineering*, 6(107), 2020.

[14] K. S. Cunningham and A. I. Gotlieb. The role of shear stress in the pathogenesis of atherosclerosis. *Laboratory Investigation*, 85:9–23, 2005.

[15] N. Baeyens, C. Bandyopadhyay, and B. G. Coon et al. Endothelial fluid shear stress sensing in vascular health and disease. *J Clin Invest.*, 126(3):812–828, 2016.

[16] Y. I. Wang, H. E. Abaci, and M. L. Shuler. Microfluidic blood-brain barrier model provides in vivo-like barrier properties for drug permeability screening. *Biotechnol. Bioeng*, 114:184–194, 2017.

[17] P. G. Saffman and G. I. Taylor. The penetration of a fluid into a porous medium or hele-shaw cell containing

a more viscous liquid. *Proc. R. Soc. A*, 245:312–329, 1958.

[18] Y. I. Wang and M. L. Shuler. Unichip enables long-term recirculating unidirectional perfusion with gravity-driven flow for microphysiological systems. *Lab Chip*, 18(2563), 2018.

[19] J. H. Sung, C. Kam, and M. L. Shuler. A microfluidic device for a pharmacokinetic–pharmacodynamic (pk–pd) model on a chip. *Lab Chip*, 10:446–455, 2010.

[20] H. E. Abaci, K. Gledhill, and Z. Guo et al. Pumpless microfluidic platform for drug testing on human skin equivalents. *Lab Chip*, 15:882–888, 2015.

[21] M. B. Esch, J.M. Prot, and Y.I. Wang et al. Multi-cellular 3d human primary liver cell culture elevates metabolic activity under fluidic flow. *Lab Chip*, 15:2269–2277, 2015.

[22] D. Moonay. What is shear rate and why is it important? *Lab Compare*, 2017.

[23] S. Dekker, W. Buesink, and M. Blom et al. Standardized and modular microfluidic platform for fast lab on chip system development. *Sensors and Actuators B*, 272:468–478, 2018.

[24] S. Dekker, P. K. Isgor, and T. Feijten et al. From chip-in-a-lab to lab-on-a-chip: a portable coulter counter using a modular platform. *Microsystems & Nanoengineering*, 4(34), 2018.

[25] S. S. Li and C. M. Cheng. Analogy among microfluidics, micromechanics, and microelectronics. *Lab Chip*, 13(3782), 2013.

[26] A. Kumar, S. Pramanik, and M. Mishra. Comsol multiphysics® modeling in darcian and non-darcian porous media. *COMSOL Conference*, 2016.

[27] A. Brosseau and A. Brouillard. Chem-eng 535: Microfluidics and microscale analysis in materials and biology. *Open Wet Ware*, 2019.

[28] T. Gao, M. Mirzadeh, and P. Bai et al. Active control of viscous fingering using electric fields. *Nature Communications*, 10(4002), 2019.

Appendix

A. Plots to investigate shear rate dependency with dimension and tilt

Figure 12 and 13 observed the shear rate when the height of channel B and when the angle of the tilt table was changed respectively. The reason why only the change in height for channel B was observed in figure 12 is because channel A already used a very small channel height of 0.25mm, and taking into consideration the fabrication limits, there was little room to make any changes. On the other hand, the height of channel B was 1.3mm, and it was possible to make it smaller if needed.

The angle was changed from 1 degree to 30 degrees in Figure 13, where the angle of tilt is in shown in radians. While 18 degrees, or 0.314 radians is approximately at 1000 reciprocal seconds for shear rate, the plot shows that it can change a lot hence tuning the shear rate by changing the tilt angle is not a very feasible option.

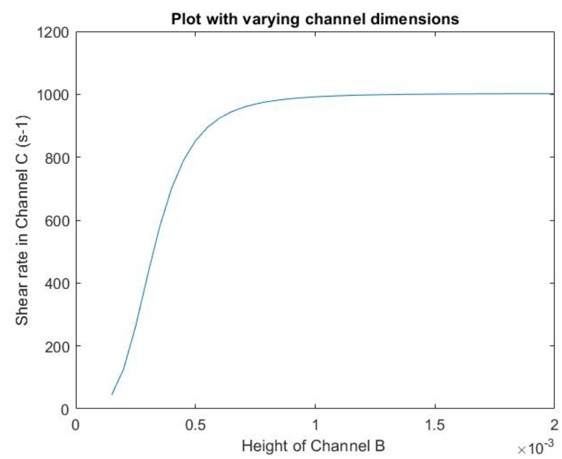

Fig. 12: Plot of Shear rate for varying height for channel B

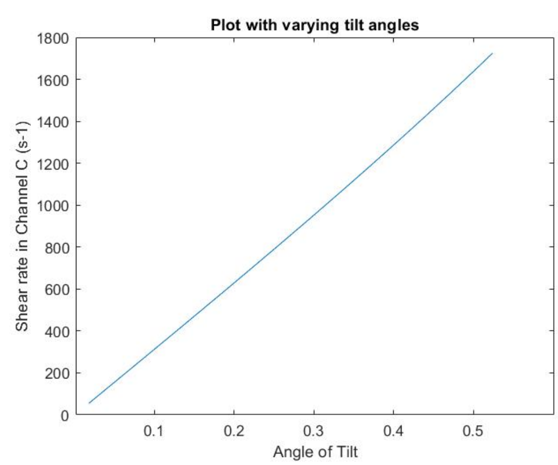

Fig. 13: Plot of Shear rate for varying Angle of Tilt

B. SolidWorks Design for calculated UniChip dimensions

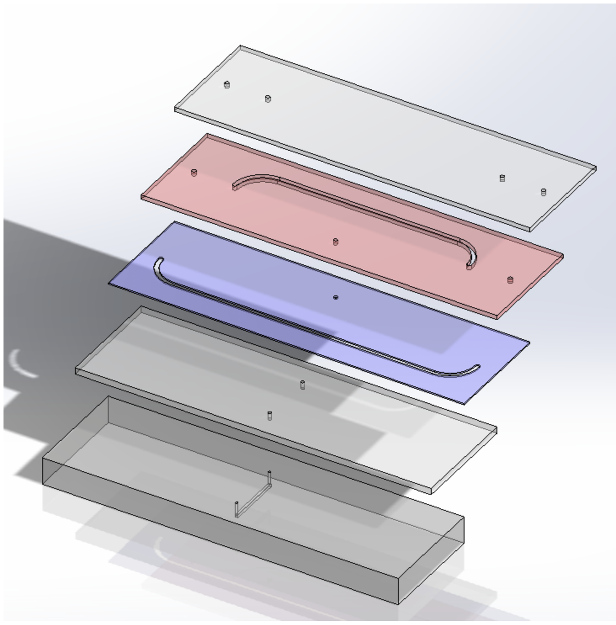

Fig. 14: Initial SolidWorks model of the UniChip implementation

C. FCB with valves for each channel to control individual flow rates

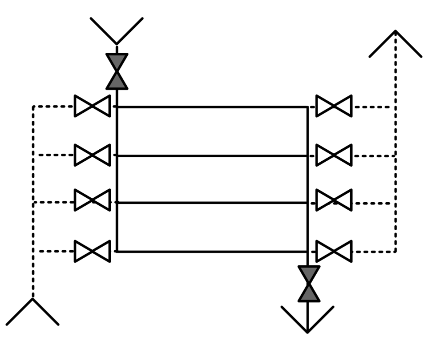

Fig. 15: Diagram of a possible implementation of VFP in FCB

The pneumatic valves will be used as a variable resistor and change the flow rate according to the channel's resultant resistance post VFP.

D. MATLAB Script

```
%%
close all
clear all
clc
%%
% 0. Introduce standardized parameters
mu = 7.9*10^-4;                %Dynamic fluid viscosity of water: Pas (30C)
rho = 994.03;                  %Fluid density of water: kgm^-3 at 35 Celsius
g = 9.8;                       %Gravitational acceleration: ms^-2
tilt = 18*pi/180;              %tilt of 18 degrees in radians


% 1. Calculate shear stress/rate for design
% 1.1 Define parameters of channels (meters)
ws_a = 1.3*10^-3;
hs_a = 0.25*10^-3;
ls_a = 15.3*10^-3;

hs_b = 1.4*10^-3;              % ws > hs
ws_b = 1.5*10^-3;
ls_b = 26.3*10^-3;

ws_c = 0.76*10^-3;
hs_c = 0.25*10^-3;
ls_c = 6.25*10^-3;

%1.2 Calculate basic variables
%1.2.1 Difference in pressure: d_Ps = rho*g*difference in height
%difference in height for a1 to a2
d_hs_a1a2 = asin(tilt)*ls_a*2;
d_Ps_a1a2 = rho*g*d_hs_a1a2;
%difference in height for a1 to b2
d_hs_a1b2 = asin(tilt)*(ls_a+ls_b);
d_Ps_a1b2 = rho*g*d_hs_a1b2;

%1.2.2 Calculate resistances of each channel
rs_a = ((12*mu*ls_a)/(ws_a*hs_a^3))*(1-(192*hs_a)/(pi^5*ws_a)*tanh((pi*ws_a)/(2*hs_a)))^-1;
rs_b = ((12*mu*ls_b)/(ws_b*hs_b^3))*(1-(192*hs_b)/(pi^5*ws_b)*tanh((pi*ws_b)/(2*hs_b)))^-1;
rs_c = ((12*mu*ls_c)/(ws_c*hs_c^3))*(1-(192*hs_c)/(pi^5*ws_c)*tanh((pi*ws_c)/(2*hs_c)))^-1;

%1.3 Compute expected flow rate as systems of equations
syms Qs_a1 Qs_a2 Qs_c
eqs_1 = d_Ps_a1a2 == Qs_a1*rs_a+Qs_a2*rs_a;
eqs_2 = d_Ps_a1b2 == Qs_a1*rs_a+Qs_c*(rs_c+rs_b);
eqs_3 = Qs_a1 == Qs_a2+Qs_c;
eqns = [eqs_1 eqs_2 eqs_3];
vars = [Qs_a1 Qs_a2 Qs_c];
[solQs_a1 solQs_a2 solQs_c] = solve(eqns,vars);
sQs_a1 = double(solQs_a1);
sQs_a2 = double(solQs_a2);
sQs_c = double(solQs_c);               %flow rate in m^3/s

sQs_a1_mulm = sQs_a1*10^9*60;          %flow rate in ul/min
sQs_a2_mulm = sQs_a2*10^9*60;
sQs_c_mulm = sQs_c*10^9 *60;

% flow rate of a1 = 586.3 ul/min
% flow rate of a2 = 117.6 ul/min
% flow rate of c  = 468.7 ul/min

%1.4 Compute shear stress and shear rate
tau_s = (6*mu*sQs_c)/(ws_c*hs_c^2);                 %Pa
gamma_s = tau_s/mu;                                 %s^-1

%Results
% tau_s*10 = 7.796 dyne/cm^2     since dyne/cm^2 = 0.1Pa
% gamma_s = 986.78 s^-1
%%
% 2. Calculate dimensions from ideal shear stress with given channel dim.
% 2.1 Calculate target shear stress from 1000^-1
gamma_i = 1000;                    %s^-1
tau_i = gamma_i*mu;                %Pa

% 2.2 Define channel dimensions (assume diameter 250um lumen formation)
di_c = 0.25*10^-3;                 % lumen channel dimensions
```

```
li_c = 10*10^-3;

% 2.3 Calculate parameters
Qi_c = (tau_i*pi*di_c^3)/(32*mu);
ri_c = (8*mu*li_c)/(pi*(di_c/2)^4);

% 2.4 Assumptions
% 2.4.1 Assume height of channel of a = diameter of c, following similar parameters from previous
hi_a = di_c;

% 2.4.3 Assume same width for channel A average of width of channel A, B in paper
% + channel width is equal for both A and B
wi_a = 1.4*10^-3;
wi_b = wi_a;

% 2.4.4 Assume width of channel B = height of channel B
hi_b = wi_b;

% 2.4.5 Identify variables
% width of channel A = channel B
% length of channel A
syms li_a;
% difference in length of channel A and B
d_li = ls_b-ls_a;
li_b = li_a+d_li;

% 2.5 Setup systems of equations:
% 2.5.1 Pressure difference
%difference in height for a1 to a2
d_hi_a1a2 = asin(tilt)*li_a*2;
d_Pi_a1a2 = rho*g*d_hi_a1a2;
%difference in height for a1 to b2
d_hi_a1b2 = asin(tilt)*(li_a+li_b);
d_Pi_a1b2 = rho*g*d_hi_a1b2;

% 2.5.2 Calculate resistances
ri_a = ((12*mu*li_a)/(wi_a*hi_a ^3))*(1-(192*hi_a)/(pi^5*wi_a)*tanh((pi*wi_a)/(2*hi_a)))^-1;
ri_b = ((12*mu*li_b)/(wi_b*hi_b ^3))*(1-(192*hi_b)/(pi^5*wi_b)*tanh((pi*wi_b)/(2*hi_b)))^-1;

syms Qi_a1 Qi_a2
eqs_1 = d_Pi_a1a2 == Qi_a1*ri_a + Qi_a2*ri_a;
eqs_2 = d_Pi_a1b2 == Qi_a1*ri_a + Qi_c*(ri_c+ri_b);
eqs_3 = Qi_a1 == Qi_a2 + Qi_c;
eqns = [eqs_1 eqs_2 eqs_3];
vars = [Qi_a1 Qi_a2 li_a];
[solQi_a1 solQi_a2 solli_a] = solve(eqns,vars);
sQi_a1 = double(solQi_a1);
sQi_a2 = double(solQi_a2);
sli_a = double(solli_a);

sQi_a1_mulm = sQi_a1*10^9*60;        %flow rate in ul/min
sQi_a2_mulm = sQi_a2*10^9*60;

% Results:
% sli_a = 0.0338 = 33.8mm, sli_b = 44.8mm therefore long channels required
% Qa1 = 428ul/min,  Qa2 = 336ul/min

%%
% 3. Vary length of channel A and B to observe the change in shear rate, tau_v = (32*mu*sQv_c)/(pi*d^3);
% 3.1 Vary A with constant delta length to observe affect shear rate
lv_a= 0.001:0.0001:0.053;
lv_b= lv_a + d_li;

d_hv_a1a2 = asin(tilt)*lv_a*2;
d_Pv_a1a2 = rho*g*d_hv_a1a2;
d_hv_a1b2 = asin(tilt)*(lv_a+lv_b);
d_Pv_a1b2 = rho*g*d_hv_a1b2;

rv_a = ((12*mu*lv_a)/(wi_a*hi_a ^3))*(1-(192*hi_a)/(pi^5*wi_a)*tanh((pi*wi_a)/(2*hi_a)))^-1;
rv_b = ((12*mu*lv_b)/(wi_b*hi_b ^3))*(1-(192*hi_b)/(pi^5*wi_b)*tanh((pi*wi_b)/(2*hi_b)))^-1;

sQv_a1 = zeros(size(lv_a));
sQv_a2 = zeros(size(lv_a));
sQv_c = zeros(size(lv_a));

for i = 1:(length(lv_a))    % solve system of equations for various lengths
    syms Qv_a1 Qv_a2 Qv_c
    eqs_1 = d_Pv_a1a2(i) == Qv_a1*rv_a(i)+Qv_a2*rv_a(i);
    eqs_2 = d_Pv_a1b2(i) == Qv_a1*rv_a(i)+Qv_c*(ri_c+rv_b(i));
    eqs_3 = Qv_a1 == Qv_a2 +Qv_c;
    eqnv = [eqs_1 eqs_2 eqs_3];
    varv = [Qv_a1 Qv_a2 Qv_c];
    [solQv_a1 solQv_a2 solQv_c] = solve(eqnv,varv);
    sQv_a1(i) = double(solQv_a1);
    sQv_a2(i) = double(solQv_a2);
    sQv_c(i) = double(solQv_c);
end

tau_v = (32*mu*sQv_c)/(pi*di_c^3);
gamma_v = tau_v/mu;

% 3.2 Varying length B/delta length with constant A
lv2_a = sli_a;
d_lv2 = 0.0005:0.0001: 0.02;
lv2_b= lv2_a + d_lv2;

d_hv2_a1a2 = asin(tilt)*lv2_a*2;
d_Pv2_a1a2 = rho*g*d_hv2_a1a2;
d_hv2_a1b2 = asin(tilt)*(lv2_a+lv2_b);
d_Pv2_a1b2 = rho*g*d_hv2_a1b2;

rv2_a = ((12*mu*lv2_a)/(wi_a*hi_a ^3))*(1-(192*hi_a)/(pi^5*wi_a)*tanh((pi*wi_a)/(2*hi_a)))^-1;
rv2_b = ((12*mu*lv2_b)/(wi_b*hi_b ^3))*(1-(192*hi_b)/(pi^5*wi_b)*tanh((pi*wi_b)/(2*hi_b)))^-1;

sQv2_a1 = zeros(size(lv2_b));
sQv2_a2 = zeros(size(lv2_b));
sQv2_c = zeros(size(lv2_b));

for i = 1:(length(lv2_b))
    syms Qv2_a1 Qv2_a2 Qv2_c
    eqs_1 = d_Pv2_a1a2 == Qv2_a1*rv2_a+Qv2_a2*rv2_a;
    eqs_2 = d_Pv2_a1b2(i) == Qv2_a1*rv2_a+Qv2_c*(ri_c+rv2_b(i));
    eqs_3 = Qv2_a1 == Qv2_a2 +Qv2_c;
    eqnv = [eqs_1 eqs_2 eqs_3];
    varv = [Qv2_a1 Qv2_a2 Qv2_c];
    [solQv2_a1 solQv2_a2 solQv2_c] = solve(eqnv,varv);
    sQv2_a1(i) = double(solQv2_a1);
    sQv2_a2(i) = double(solQv2_a2);
    sQv2_c(i) = double(solQv2_c);
end

tau_v2 = (32*mu*sQv2_c)/(pi*di_c^3);
gamma_v2 = tau_v2/mu;

figure;
plot(lv_a, gamma_v);
set(gca,'XTick',(0:0.01:0.06))

hold on
plot (lv2_b, gamma_v2);

xlabel('Length of Channel A and B (m) ')
ylabel('Shear rate in Channel C (s-1)')
title('Plot with varying channel dimensions')
legend ('Varying L_a with same \Delta length', 'Varying L_b with L_a = 33.8mm', 'Location','southeast')

hold off

% 3.3 Varying height of Channel B to observe effect to shear rate
lv3_a = sli_a;
lv3_b= lv3_a + d_li;

hv3_b = 150*10^-6:50*10^-6:2*10^-3;
wv3_b = hv3_b;

d_hv3_a1a2 = asin(tilt)*lv3_a*2;
d_Pv3_a1a2 = rho*g*d_hv3_a1a2;
d_hv3_a1b2 = asin(tilt)*(lv3_a+lv3_b);
d_Pv3_a1b2 = rho*g*d_hv3_a1b2;

rv3_a = ((12*mu*lv3_a)/(wi_a*hi_a^3))*(1-(192*hi_a)/(pi^5*wi_a)*tanh((pi*wi_a)/(2*hi_a)))^-1;

rv3_b = zeros(size(hv3_b));
sQv3_a1 = zeros(size(hv3_b));
sQv3_a2 = zeros(size(hv3_b));
```

```
sQv3_c = zeros(size(hv3_b));

for i = 1:(length(hv3_b))
    rv3_b(i) = ((12*mu*lv3_b)/(wv3_b(i)*hv3_b(i)^3))*(1-(192*hv3_b(i))/(pi^5*wv3_b(i))*tanh((pi*wv3_b(i))/(2*hv3_b(i))))^-1;
    syms Qv3_a1 Qv3_a2 Qv3_c
    eqs_1 = d_Pv3_a1a2 == Qv3_a1*rv3_a+Qv3_a2*rv3_a;
    eqs_2 = d_Pv3_a1b2 == Qv3_a1*rv3_a+Qv3_c*(ri_c+rv3_b(i));
    eqs_3 = Qv3_a1 == Qv3_a2 +Qv3_c;
    eqnv = [eqs_1 eqs_2 eqs_3];
    varv = [Qv3_a1 Qv3_a2 Qv3_c];
    [solQv3_a1 solQv3_a2 solQv3_c] = solve(eqnv,varv);
    sQv3_a1(i) = double(solQv3_a1);
    sQv3_a2(i) = double(solQv3_a2);
    sQv3_c(i) = double(solQv3_c);
end

tau_v3 = (32*mu*sQv3_c)/(pi*di_c^3);
gamma_v3 = tau_v3/mu;

figure;
plot(hv3_b, gamma_v3);
set(gca,'XTick',(0:0.5*10^-3:2.2*10^-3))
xlabel('Height of Channel B ')
ylabel('Shear rate in Channel C (s-1)')
title('Plot with varying channel dimensions')

%%
% 4. Sweep angle between 1 to 30 degrees to observe the change in flow
la_a = sli_a;
la_b= la_a + d_li;

tilt_a = 1*pi/180:1*pi/180:30*pi/180;

d_ha_a1a2 = asin(tilt_a)*la_a*2;
d_Pa_a1a2 = rho*g*d_ha_a1a2;
d_ha_a1b2 = asin(tilt_a)*(la_a+la_b);
d_Pa_a1b2 = rho*g*d_ha_a1b2;

ra_a = ((12*mu*la_a)/(wi_a*hi_a ^3))*(1-(192*hi_a)/(pi^5*wi_a)*tanh((pi*wi_a)/(2*hi_a)))^-1;
ra_b = ((12*mu*la_b)/(wi_b*hi_b ^3))*(1-(192*hi_b)/(pi^5*wi_b)*tanh((pi*wi_b)/(2*hi_b)))^-1;

sQa_a1 = zeros(size(tilt_a));
sQa_a2 = zeros(size(tilt_a));
sQa_c = zeros(size(tilt_a));

for i = 1:(length(tilt_a))
    syms Qa_a1 Qa_a2 Qa_c
    eqs_1 = d_Pa_a1a2(i) == Qa_a1*ra_a+Qa_a2*ra_a;
    eqs_2 = d_Pa_a1b2(i) == Qa_a1*ra_a+Qa_c*(ri_c+ra_b);
    eqs_3 = Qa_a1 == Qa_a2 +Qa_c;
    eqnv = [eqs_1 eqs_2 eqs_3];
    varv = [Qa_a1 Qa_a2 Qa_c];
    [solQa_a1 solQa_a2 solQa_c] = solve(eqnv,varv);
    sQa_a1(i) = double(solQa_a1);
    sQa_a2(i) = double(solQa_a2);
    sQa_c(i) = double(solQa_c);
end

tau_a = (32*mu*sQa_c)/(pi*di_c^3);
gamma_a = tau_a/mu;

figure;
plot(tilt_a, gamma_a);
set(gca,'XTick',(0:0.1:30.5*pi/180))
xlabel('Angle of Tilt')
ylabel('Shear rate in Channel C (s-1)')
title('Plot with varying tilt angles')
```